

Spectral-Domain Analysis of *E*-Plane Waveguide to Microstrip Transitions

T. Q. HO AND YI-CHI SHIH, MEMBER, IEEE

Abstract — The spectral-domain technique and a residue calculus theorem are used to compute the input impedance of a microstrip transition to a rectangular waveguide. The transition consists of a printed circuit board inserted into a waveguide housing along the *E* plane. The effects of the dielectric layer are considered in the present analysis. The behavior of the input impedance of the transition is studied with respect to the critical dimensions of the probe length and backshort location. Calculated results by the new formulation agree well with those computed using an integral equation and those measured at *Ka*-band frequencies.

I. INTRODUCTION

IN MANY microwave planar and quasi-planar circuit applications, it is often necessary to combine a waveguide circuit with a microstrip line circuit. One of the most widely used ways is the *E*-plane waveguide to microstrip line transition shown in Fig. 1. This transition consists of a printed probe on one side of the circuit board inserted into a rectangular waveguide. A waveguide backshort is placed behind the probe to maximize the power from the waveguide to the microstrip line circuit. The *E*-plane transition is attractive because of its simple structure, tuning flexibility, and broad-band performance.

Early work on the theory of waveguide to coaxial line transitions has utilized the waveguide Green's function and sinusoidal current distribution for the input impedance calculations [1]–[4]. Both touching and nontouching cases were considered. In the past, the waveguide to microstrip transitions have been designed based on these analyses because of the geometrical similarities. Due to the approximation, fine tuning is always required for broad-band performance. As the operating frequency becomes higher, the design based on the approximation becomes less accurate because of the more pronounced dielectric layer effects. Therefore, a more rigorous approach, one that takes into account the dielectric effects, is essential for millimeter-wave applications.

This paper presents an analytical approach for computing the input impedance of an *E*-plane waveguide to microstrip transition. The formulation combines the spectral-domain technique [5] with a residue calculus theorem [6] utilizing a self-reaction concept to calculate the power

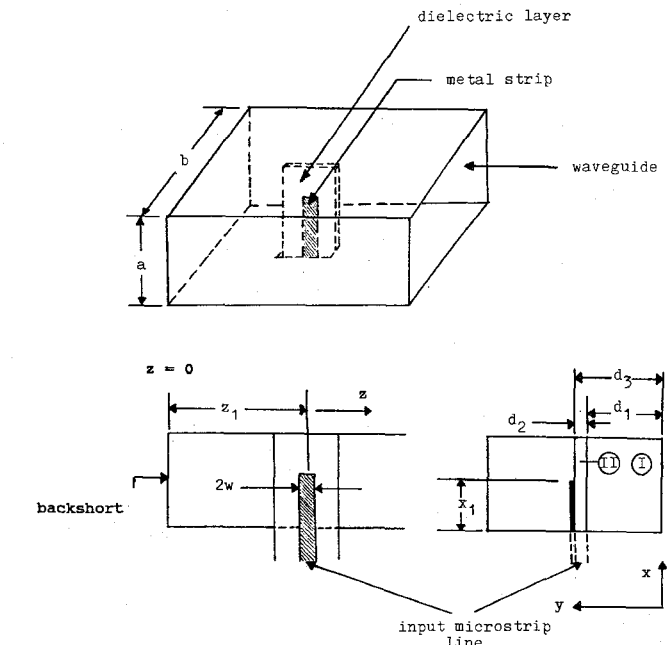


Fig. 1. Geometry of an *E*-plane waveguide to microstrip transition.

radiated from the probe into the rectangular waveguide. Compared to the space-domain integral equation technique, the present method is preferred because of the closed-form spectral-domain Green's function and simple algebraic equations involved. The dielectric layer is easily incorporated into the formulation of the Green's function.

The behavior of the input impedance of the transition is studied with respect to the critical dimensions of probe length and backshort location. The computed results for an air-dielectric case ($\epsilon_r = 1.0$) agree well with those obtained by the integral equation technique. Based on the numerical calculations, several *Ka*-band transitions have been designed and tested. Good agreement on the input *VSWR* has been obtained between the measurement and the theory.

II. FORMULATION

Fig. 1 shows the geometry of an *E*-plane waveguide to microstrip transition where a printed circuit is mounted inside a dominant TE_{10} waveguide. Perfect ground planes formed by the waveguide walls are located at $x = 0$ and a , $y = 0$ and b , and $z = 0$. For simplicity of analysis, we

Manuscript received January 21, 1988; revised July 26, 1988.

T. Q. Ho is with the Space and Communications Group, Hughes Aircraft Company, P.O. Box 92919, Los Angeles, CA 90009.

Y.-C. Shih is with the Industrial Electronics Group, Hughes Aircraft Company, P.O. Box 2940, Torrance, CA 90509.

IEEE Log Number 8824986.

assumed that the dielectric slab with thickness d_2 is uniformly extended throughout the waveguide, and also the current strip is infinitely thin in the y direction and narrow in the transverse direction with respect to the metal strip, so that the current in the z direction is neglected.

In the spectral-domain technique, the input impedance of the E -plane transition Z_{in} seen by the microstrip line is obtained through the self-reaction concept of the following equation:

$$Z_{\text{in}} = -\frac{1}{I_{\text{in}}^2} \left(\sum_{n=0}^{\infty} \sum_{m=1}^{\infty} \int_0^{\infty} \tilde{E}_x(\alpha, \gamma, \beta) \cdot \tilde{J}_x(\alpha, \gamma, \beta) d\beta \right). \quad (1)$$

The quantities with a tilde (\sim) are the Fourier transforms of the corresponding quantities. The product $\tilde{E}_x(\alpha, \gamma, \beta) \cdot \tilde{J}_x(\alpha, \gamma, \beta)$ represents the power radiated within the confines of the waveguide walls; α , γ , and β are the transformation variables of x , y , and z . I_{in} is the total input current at the reference plane $x = 0$. $\tilde{E}_x(\alpha, \gamma, \beta)$ and $\tilde{J}_x(\alpha, \gamma, \beta)$ represent the x -directed electric field and current distribution, respectively. $\tilde{E}_x(\alpha, \gamma, \beta)$ is derived through the dyadic Green's function $\tilde{G}_{xx}(\alpha, \gamma, \beta)$ and the current distribution $\tilde{J}_x(\alpha, \gamma, \beta)$:

$$\tilde{E}_x(\alpha, \gamma, \beta) = \tilde{G}_{xx}(\alpha, \gamma, \beta) \cdot \tilde{J}_x(\alpha, \gamma, \beta) \quad (2a)$$

where

$$\tilde{G}_{xx}(\alpha, \gamma, \beta) = \frac{\beta^2}{\alpha^2 + \beta^2} Z^e + \frac{\alpha^2}{\alpha^2 + \beta^2} Z^h. \quad (2b)$$

Z^e and Z^h are the eigenvalue equations of the LSE and LSM modes. Both quantities can be arrived at through the transverse resonance condition, as follows:

$$Z^e = \left(\frac{\hat{Y}_1}{\gamma_1} \coth \gamma_1 d_1 + \frac{\hat{Y}_2}{\gamma_2} \cdot \frac{\frac{\hat{Y}_1}{\gamma_1} \coth \gamma_1 d_1 \coth \gamma_2 d_2 + \frac{\hat{Y}_2}{\gamma_2}}{\frac{\hat{Y}_1}{\gamma_1} \coth \gamma_1 d_1 + \frac{\hat{Y}_2}{\gamma_2} \coth \gamma_2 d_2} \right)^{-1} \quad (3a)$$

$$Z^h = \left(\frac{\gamma_1}{\hat{Z}_1} \coth \gamma_1 d_1 + \frac{\gamma_2}{\hat{Z}_2} \cdot \frac{\frac{\gamma_1}{\hat{Z}_1} \coth \gamma_1 d_1 \coth \gamma_2 d_2 + \frac{\gamma_2}{\hat{Z}_2}}{\frac{\gamma_1}{\hat{Z}_1} \coth \gamma_1 d_1 + \frac{\gamma_2}{\hat{Z}_2} \coth \gamma_2 d_2} \right)^{-1} \quad (3b)$$

Here d_1 , d_2 , \hat{Y}_1 , \hat{Y}_2 , \hat{Z}_1 , and \hat{Z}_2 are the thickness, admittivity, and impedivity of regions 1 and 2, respectively. The quantities γ_1 and γ_2 are the propagation constants in the y direction and can be derived through the characteristic equation

$$\alpha_n^2 + \beta_{mn}^2 = \omega^2 \epsilon_0 \mu_0 \epsilon_r + \gamma_{im}^2, \quad i=1,2 \quad (4)$$

where ϵ_r is the relative dielectric constant of region 2, ω is the angular frequency, and m and n are the mode index numbers. $\tilde{J}_x(\alpha, \gamma, \beta)$ is obtained through the Fourier transformation of a sinusoidal wave with appropriate applied

boundary conditions [7]. An application of image theory [8] is used to expand $\tilde{J}_x(\alpha, \gamma, \beta)$ into the final expression:

$$\tilde{J}_x(\alpha, \gamma, \beta) = j \frac{4J_0}{\beta} \sin \left(\frac{m\pi d_3}{b} \right) \sin(\beta z_1) \sin(\beta w) \cdot \frac{k}{k^2 - \alpha^2} (\cos(\alpha x_1) - \cos(kx_1)). \quad (5)$$

Here z_1 is the backshort location, and x_1 and w are the length and width of the metal strip, respectively. J_0 is the magnitude of the input current, k is the medium wavenumber, and d_3 is the distance between the metal strip and $y = 0$ in the transverse direction.

Since poles exist in the right-hand side of (3a) and (3b), equation (1) must be further formulated to yield its simplified expression. To evaluate the product $\tilde{E}_x(\alpha, \gamma, \beta) \cdot \tilde{J}_x(\alpha, \gamma, \beta)$, the discrete value of β_{mn} must first be determined from the dyadic Green's function $\tilde{G}_{xx}(\alpha, \gamma, \beta)$. Once β_{mn} has been obtained, the complex residue theorem can be applied to (1) to compute the input impedance Z_{in} :

$$Z_{\text{in}} = \lim_{\beta \rightarrow \beta_{mn}} (\beta - \beta_{mn}) \left[\sum_{n=0}^{\infty} \sum_{m=1}^{\infty} -\frac{2j}{\sin^2(kx_1)} \left(\frac{\sin(\beta w)}{\beta w} \right)^2 \cdot \sin(\beta z_1) \sin^2 \left(\frac{m\pi d_3}{b} \right) (\cos(\alpha x_1) - \cos(kx_1))^2 \cdot \frac{e^{j\beta z_1}}{a} \left(\frac{k}{k^2 - \alpha^2} \right)^2 \left(\frac{\beta^2}{\alpha^2 + \beta^2} Z^e + \frac{\alpha^2}{\alpha^2 + \beta^2} Z^h \right) \right]. \quad (6)$$

The input *VSWR* at the reference plane $x = 0$ is determined as follows:

$$\text{VSWR} = \frac{1 + \sqrt{\frac{(R_{\text{in}} - Z_0)^2 + X_{\text{in}}^2}{(R_{\text{in}} + Z_0)^2 + X_{\text{in}}^2}}}{1 - \sqrt{\frac{(R_{\text{in}} - Z_0)^2 + X_{\text{in}}^2}{(R_{\text{in}} + Z_0)^2 + X_{\text{in}}^2}}}. \quad (7)$$

Z_0 is the characteristic impedance of the input microstrip line, and R_{in} and X_{in} are the real and imaginary parts of Z_{in} .

III. RESULTS

In verifying our calculations, the standard *Ka*-band waveguide dimensions are used to compute the input impedance of the transition. The quantities d_3 and w are fixed at 3.5 mm and 0.187 mm, respectively. The large values of m and n are chosen so as to ensure the convergence of the input impedance. Fig. 2 shows the numerical data obtained from the spectral-domain approach and Collin's method [2] for an air-dielectric case ($\epsilon_r = 1.0$). The backshort location z_1 and the probe length x_1 are fixed at 2.8 mm and 2.1 mm, respectively. Data computed by the two methods show good agreement in the input impedance of the transition calculated from 27.0 and 40.0 GHz. The input resistance reaches its maximum at approximately 36.0 GHz, and the reactance remains capacitive through-

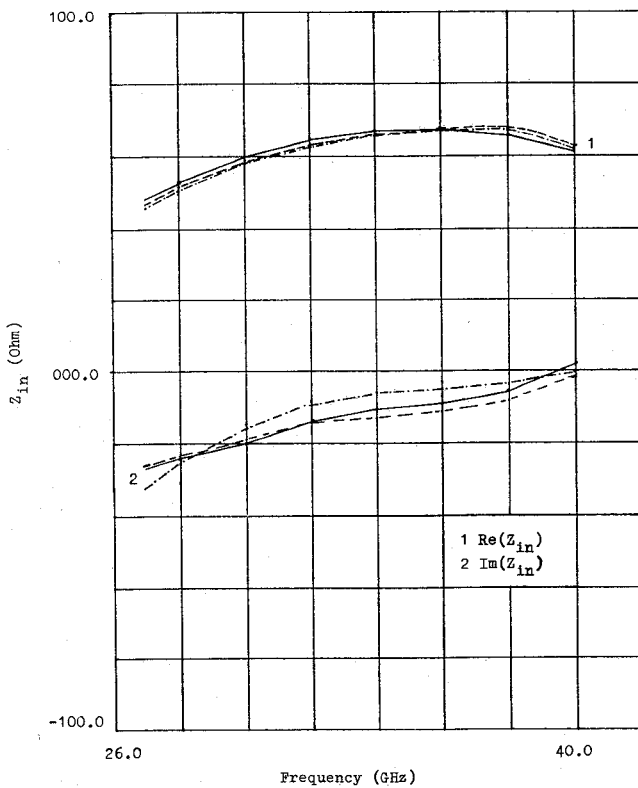


Fig. 2. Input impedance versus frequency. E -plane transition with $x_1 = 2.1$ mm, $z_1 = 2.8$ mm, $d_3 = 3.5$ mm, $w = 0.187$ mm, and $\epsilon_r = 1.0$. —···— Spectral domain technique. - - - Collin's method [2]. — Integral equation technique.

out frequencies. Data obtained by the integral equation technique using the current source are also presented in the same figure for comparison.

In this set of computations, all parameters are fixed at a constant value except for the relative dielectric constant. With the exception of d_3 being 3.63 mm, all physical dimensions are the same as in the previous case. A 10-mil-thick substrate is used for the dielectric layer. Fig. 3 shows the dominant mode impedance of an E -plane waveguide to microstrip transition for the cases of air ($\epsilon_r = 1.0$), Duroid ($\epsilon_r = 2.2$), and quartz ($\epsilon_r = 3.78$), which are used for the dielectric slab. The study shows that the reactance changes from inductive to capacitive at resonance. This response differs from the case of the total input reactance, in which a positive reactance slope is obtained. The input impedance lowers the resonant frequency for a higher dielectric constant. This behavior is expected because of higher β_{mn} . The characteristic of the input impedance of the E -plane waveguide to microstrip transition is then further studied for a number of cases with Duroid substrate. Fig. 4 shows the computed input impedance of the E -plane transition for four different cases. Here z_1 is fixed to be constant, and x_1 is varied from 1.6 to 2.2 mm in order to observe the frequency response of the input impedance. The resistive part of the input impedance increases almost linearly with the magnitude of x_1 while the resonant frequency of the input reactance shifts toward the lower end of the waveguide band. Fig. 5 shows how the

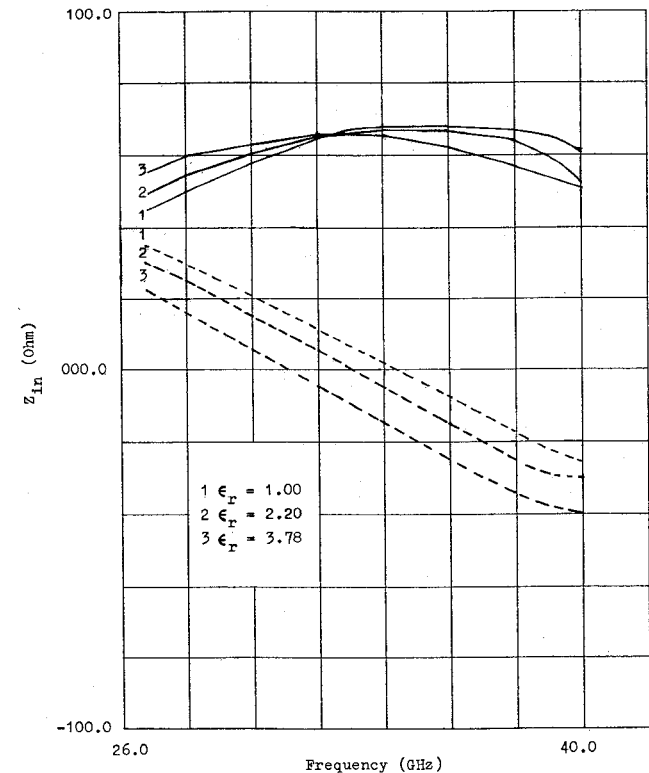


Fig. 3. Dominant mode impedance versus frequency as a function of ϵ_r . E -plane transition with $x_1 = 2.1$ mm, $z_1 = 2.8$ mm, $d_3 = 3.63$ mm, and $w = 0.187$ mm. — $\text{Re}(Z_{\text{in}})$. - - - $\text{Im}(Z_{\text{in}})$.

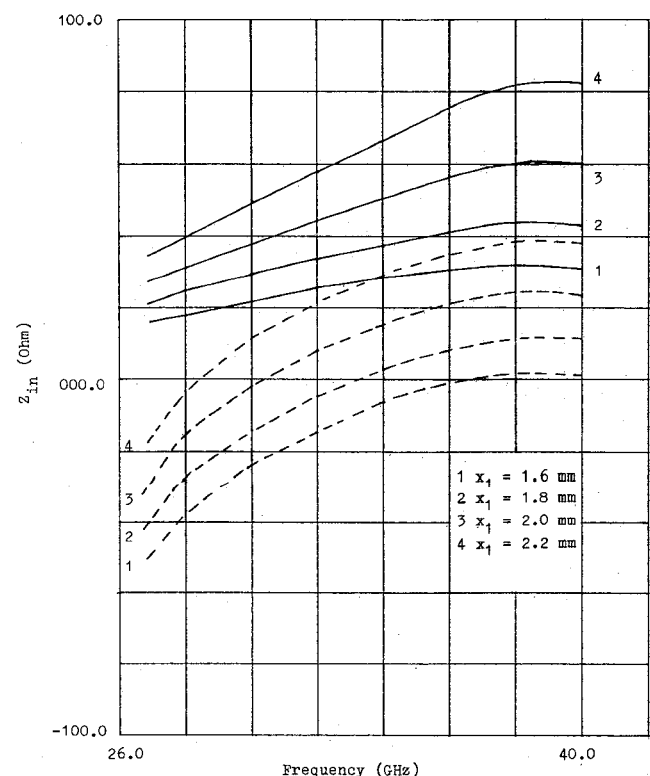


Fig. 4. Input impedance versus frequency as a function of x_1 . E -plane transition with $z_1 = 2.0$ mm, $d_3 = 3.63$ mm, $w = 0.187$ mm, and $\epsilon_r = 2.2$. — $\text{Re}(Z_{\text{in}})$. - - - $\text{Im}(Z_{\text{in}})$.

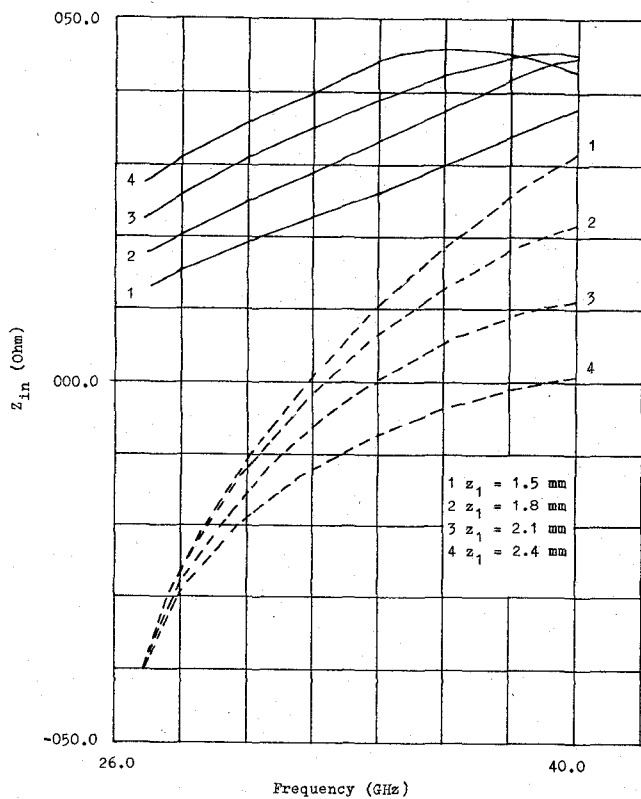


Fig. 5. Input impedance versus frequency as a function of z_1 . E -plane transition with $x_1 = 1.8$ mm, $d_3 = 3.63$ mm, $w = 0.187$ mm, and $\epsilon_r = 2.2$. — $\text{Re}(Z_{\text{in}})$. - - - $\text{Im}(Z_{\text{in}})$.

input impedance changes with frequency as a function of the backshort location z_1 . The quantity x_1 is chosen to be 1.8 mm and w is also fixed at 0.187 mm. In these cases, z_1 is varied from 1.5 mm to 2.4 mm and a family of curves is generated. As the backshort moves farther from the center of the microstrip probe, we observe that the frequency which indicates the maximum radiation moves toward the lower edge of the waveguide band as the reactive part of the impedance lowers its saturation level. The input reactance is more sensitive to the variation of z_1 in the upper half of the Ka -band.

In the experimental study, a chemical etching technique was used for fabricating the transitions on 10-mil-thick Duroid substrates. The printed circuit was then mounted on a general-purpose split block test fixture for RF evaluation. Fig. 6 shows the configuration of a Ka -band waveguide to microstrip transition embedded inside the test fixture. The exciting aperture is small and its effect on the input impedance is relatively insignificant. We used the reflection coefficient instead of directed Z_{in} measurement because of the difficulties involved in obtaining a Ka -band vector network analyzer and in developing a de-embedding technique to extract measured S parameters. The dimensions of the transition were obtained through the evaluation of (7). Z_0 was chosen to be 70.0Ω . Fig. 7 shows the calculated and typical measured input $VSWR$ of an E -plane waveguide to microstrip transition when $x_1 = 2.0$ mm, $z_1 = 2.5$ mm, $d_3 = 3.63$ mm, $w = 0.187$ mm, and $\epsilon_r = 2.2$ are used as the parameters. The data show that a

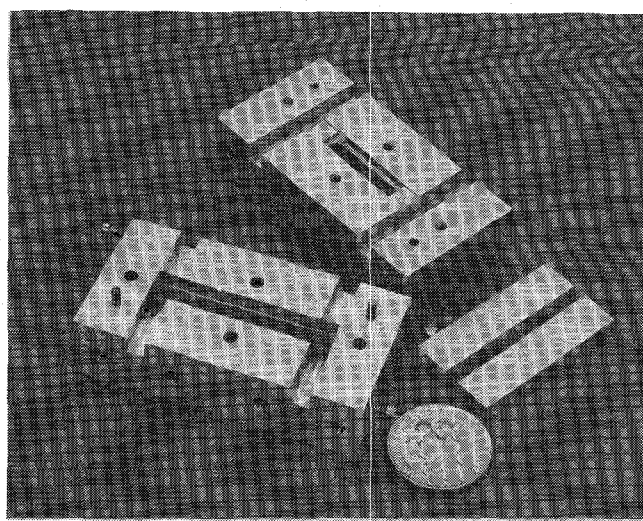


Fig. 6. Ka -band waveguide to microstrip transition circuit.

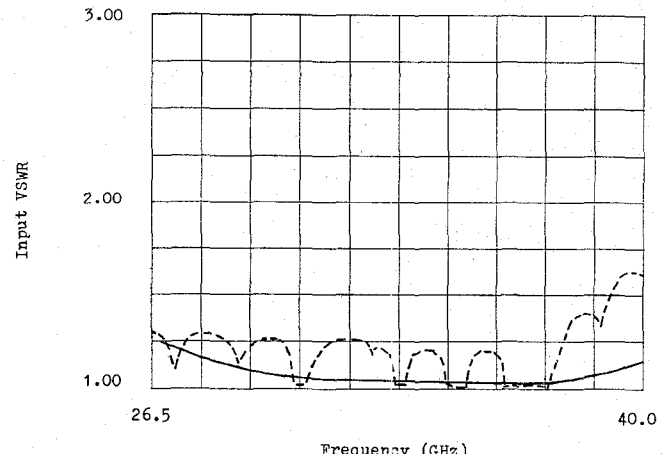


Fig. 7. Input $VSWR$ versus frequency. E -plane waveguide to microstrip transition with $x_1 = 2.0$ mm, $z_1 = 2.5$ mm, $d_3 = 3.63$ mm, $w = 0.187$ mm, and $\epsilon_r = 2.2$. — Theoretical. - - - Experimental.

value of 1.28 or better was achieved over most of the waveguide band. Numerical results obtained by the spectral-domain technique in general agree reasonably well with the experimental data.

IV. CONCLUSION

The spectral-domain technique and a residue calculus theorem have been applied to the analysis of a waveguide excitation problem. The formulation utilizes a self-reaction concept to calculate the input impedance of the structure. The analysis takes into account the dielectric layer effect, which is important in high-frequency applications. Various cases are studied with respect to the probe length and the backshort location. The new formulation yields numerical results agreeing well with those computed using the integral equation technique and those measured at Ka -band frequencies.

REFERENCES

[1] W. Z. Chien, L. Infeld, J. R. Pounder, A. F. Steveson, and J. L. Synge, "Contributions to theory of waveguide," *Can. J. Res., Sect. A*, vol. 27, pp. 69-129, 1949.

- [2] R. E. Collin, *Field Theory of Guided Waves*. New York: McGraw-Hill, 1960, ch. 7, pp. 258-307.
- [3] R. F. Harrington, *Time Harmonic Electromagnetic Field*. New York: McGraw-Hill, 1961, ch. 8, pp. 381-440.
- [4] R. L. Eischenhart and P. J. Khan, "Theoretical and experimental analysis of a waveguide mounting structure," *IEEE Trans. Microwave Theory Tech.*, vol. MTT-19, pp. 706-719, 1971.
- [5] T. Itoh, "Spectral domain admittance approach for dispersion characteristics of generalized printed transmission lines," *IEEE Trans. Microwave Theory Tech.*, vol. MTT-28, pp. 733-736, 1980.
- [6] Q. Zhang and T. Itoh, "Spectral-domain analysis of scattering from E-plane circuit elements," *IEEE Trans. Microwave Theory Tech.*, vol. MTT-35, pp. 138-150, 1987.
- [7] K. Chang and P. J. Khan, "Analysis of a narrow capacitive strip in waveguide," *IEEE Trans. Microwave Theory Tech.*, vol. MTT-22, pp. 536-541, 1974.
- [8] W. L. Stutzman and G. A. Thiele, *Antenna Theory and Design*. New York: Wiley, 1981, ch. 2, pp. 87-92.

†



T. Q. Ho was born on January 11, 1961, in Saigon, Vietnam. He received the B.S.E.E. degree from Pennsylvania State University, University Park, in 1983 and the M.S.E.E. degree from California State University, Northridge, in 1987.

Prior to joining Hughes Aircraft Company in 1984, he was a microwave circuit design engineer at Stable Energy Sources, Lancaster, PA. At Hughes Torrance Research Center, he has been involved in the research and development of advanced millimeter-wave integrated circuits

based on FET's. Currently, he is a Senior Member of the Technical Staff at Hughes Space & Communications Group, where he is engaged in the development of flight RF modules and subsystems. His designing experience has included DRO's, VCO's, LNA's, filters, couplers, power dividers, and phase shifters. His present research interest is in solving waveguide excitation problems using numerical methods.

‡



Yi-Chi Shih (S'80-M'82) was born in Taiwan, Republic of China. He received the B.Sc. degree from the National Taiwan University, Taiwan, in 1976, the M.Sc. degree from the University of Ottawa, Ontario, Canada, in 1980, and the Ph.D. degree from the University of Texas at Austin in 1982, all in electrical engineering.

In September 1982, he joined the faculty at the Naval Postgraduate School, Monterey, CA, as an Adjunct Professor of Electrical Engineering. From April 1984 to May 1986, he was with the

Hughes Aircraft Company, Microwave Products Division, Torrance, CA, as a Member of the Technical Staff. From May 1986 to May 1987, he was the Technical Director at MM-Wave Technology, Inc., Torrance, CA. Since May 1987, he has been an independent technical consultant. His research interests include the application of numerical techniques to electromagnetic field problems and the modeling and development of millimeter-wave MIC and MMIC circuits.